

## ***Response to Reviewer #1***

*Kim et al. present the calibration of the broad supersaturation scanning CCN instrument. The instrument is a modified version of the DMT CCN, where the aerosol is entering the growth tube in a spatially distributed manner. As a result, particles experience a range of supersaturation. When fed with monodisperse particles, the activated fraction can be related directly to the hygroscopicity parameter of the aerosol at that size. The manuscript presents experimental calibration data for this instrument. Comparison with regular size-resolved CCN measurements shows reasonable agreement in the derived kappa for the two methods.*

*Overall the paper is well written. The method is clever and promises a faster time-response measurement with relatively small modifications to an existing widely available commercial instrument. The manuscript is relevant to the readers of AMT and I recommend publication if the following comments can be addressed.*

A: We thank the reviewer for helpful comments on our manuscript. We expect our manuscript to improve more qualitatively when your comments are reflected. Below each of questions/comments is written first with the *Italic font*, and then our response is followed with the normal font. We marked newly added or revised sentences by highlighting them in the revised manuscript.

### **Major comments.**

*Q1: Influence of multiply charged particles: The authors select the most optimistic scenario to conclude that the effect of multiply charged particles is small. Conditions of lower supersaturation and larger mode diameter will have a much more significant influence of multiply charged particles. Figure 4 should include  $s = 0.1\%$  and  $D_g = 150\text{ nm}$  to bound the magnitude of the effect, which may be especially relevant in some ambient cases scenarios.*

A: As you suggested, we calculated ideal activation fraction with assumed atmospheric-relevant log-normal particle size distribution. As we think 150 nm of  $D_g$  is too large and  $D_g$  of many cases is less than 100nm, we adopted particle number size distribution from Rose et al. (2011) with  $N = 1000\text{ cm}^{-3}$ ,  $D_g = 80\text{ nm}$ , and  $\sigma_g = 1.5$ . As the BS2-CCNC uses the  $S_{tube}$  distribution in the chamber, not a single supersaturation, the supersaturation is too low in the edge of chamber if we set 0.1% for  $S_{max}$ . Therefore, we set 0.2% for  $S_{max}$ , instead of 0.1. Additionally, we assumed aerosols with  $\kappa$  of 0.3 are internally mixed. According to the Fig. R1,  $F_{act\_double}$  is up to 0.05 implying that the effect of doubly charged particle is not that significant but we still need to consider the effect of doubly charged particle for ambient aerosol measurement if  $D_g$  or  $\sigma_g$  becomes large. As Section 3 is focused on the calibration experiment, we added this result in Supplement (Figure S4) and sentence “Assuming the atmospheric relevant particle number size distribution with  $N = 1000\text{ cm}^{-3}$ ,  $D_g = 80\text{ nm}$ , and  $\sigma_g = 1.5$  from Rose et al. (2011),  $F_{act\_double}$  is up to 0.05 (Fig. S4). It is noted that aerosols with  $\kappa$  of 0.3 is assumed to be internally mixed, and  $S_{max}$  is set to be 0.2%. Although the effect of doubly charged particle in Fig. S4 is not significant, the effect of doubly charged particle cannot be ignored if  $D_g$  or  $\sigma_g$  becomes large in specific environments or conditions.” (Line 200-204).

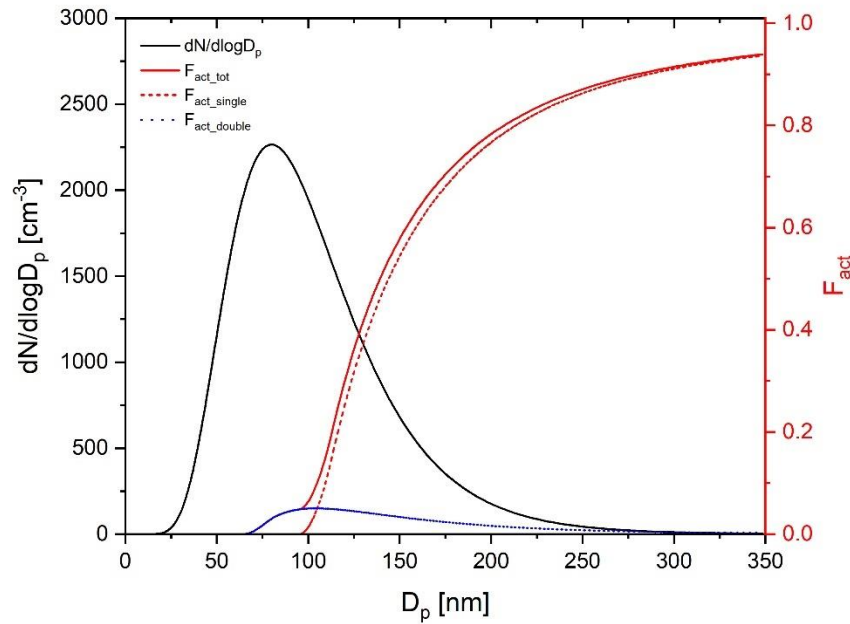


**Figure R 1:** Calculated ideal activation fraction for log-normally distributed, charge-equilibrated particles transmitted BS2-CCNC system. Shown are assumed particle size distribution (black-solid line, left ordinate,  $N = 1000 \text{ cm}^{-3}$ ,  $D_g = 80 \text{ nm}$ , and  $\sigma_g = 1.5$ ), total activation fraction (red solid line), activation fractions by singly charged particle (red dashed line) and doubly charged particle (blue dashed line). It is noted that  $S_{max}$  is set to be 0.2% in this calculation.

*Q2: Time resolution: The promise of the technique is that kappa can be measured at much higher time resolution. However, the manuscript does not really show this very well.*

*Figure 11 shows temporally averaged data. Perhaps this is necessary because the 1 min data are too noisy? If that is the case, it would undercut the argument of improved time resolution.*

*Related, there is a concern on what went into the average. Technically, the comparison should be for the size closest to the activation diameter of the size resolved CCN, which changes with time. The authors should be more precise when matching the kappa values in the comparison (i.e. only include +/- 1 size bin in their kappa inter-comparison).*

*In general, the authors should discuss time resolution in a more nuanced manner. When pressed, scanning flow CCN and scanning mobility CCN can find an activation spectrum in 30s to 1 min time, which would provide a kappa value every minute. The D50/supersaturation could be adjusted by changing the flow rate after each scan. This may be inferior to finding the kappa value at a fixed size which the BS2 technique does. However, at face value the time resolution of what can be achieved with traditional methods would seem much more similar to what is achieved in this work, although that setup might be easily improved by changing the configuration (see below). Related, it would be good to add discussion on the minimum time needed to get a kappa measurement. Why was 1 min selected? What determines the quality of the measurement? Is it the number of counts? If so can this value be specified? In principle, it would seem possible to run the system with a continuously scanning DMA (e.g. a 3 min SMPS scan) and then report the kappa data in a few discrete size bins. The feasibility of such an approach would depend on the time required to obtain a good kappa characterization. The authors should provide detailed comments on what may or may not be possible with this technique.*

A: For Fig.11, we use 1 min averaged data to not only compare the  $\kappa$  value between DMA-CCN and BS2-CCN measurement but also obtain more reliable result from both measurements. Instrumental setup for inter-comparison experiment is on Fig.S6. It doesn't mean that 1 minute is the minimum time resolution to obtain  $\kappa$  from BS2-CCN system.

For detailed analysis of time resolution of BS2-CCN system, we added a figure of exemplary  $D_p$  scan with ammonium sulfate ( $D_p$ : 20 – 100 nm,  $dT= 10$  K). We change diameter every 40 seconds and plot each of 1 second data (Figure. R2, Figure S2 in the supplement). For scanning, it takes about 10 seconds (maximum) to stabilize immediately after changing the particle size. We then averaged the 30-second data and display the average and standard deviation value of each dry diameter in orange together in Fig. R2a. The details of average and standard deviation value of each dry diameter are presented in Table R1. Additionally, we calculated the absolute deviation value for each data. The absolute deviations increased during the stabilization especially when CCN number concentration starts to increase. After stabilization, absolute deviation was mostly less than 0.05 except when  $F_{act}$  value is higher than 0.85. It is noted that we exclude the data which  $F_{act}$  is higher than 0.85 for analysis (Line 295 – 296). In other words, we could get reliable  $\kappa$  value in 1 second time resolution after stabilization as  $\kappa$  value is derived from  $F_{act}$  directly. We also presented  $\kappa$  distribution which corresponds to the  $F_{act}$  value of particle ranged from 50 nm to 150 nm in Fig.S4. Although we need to consider the stabilization time (~10s) after changing particle size for scanning measurement, we could derive  $\kappa$  value in 1 second if we set a single particle size implying that it is applicable to aircraft measurement which requires high-time resolution. Also, BS2-CCN system minimize the potential problem of aerosol volatilization and technical complexity as the BS2-CCN system uses constant temperature gradient and flow rate.

We add Fig. R2 in supplement information (Figure S2 in the Supplement) and sentences “Figure S2 is an exemplary  $D_p$  scan with ammonium sulfate particle to examine the time resolution of BS2-CCN system.  $F_{act}$  of each diameter is measured every 40 seconds including stabilization. It is noted that  $N_{CN}$  and  $N_{CCN}$  data has 1s time resolution and thereby  $F_{act}$  data with 1s time resolution are initially available. For scanning, it takes up to 10 seconds to stabilize immediately after changing the particle size. Absolute deviation of  $F_{act}$  is mostly less than 0.05 except when  $F_{act}$  is higher than 0.85. In other words, we could get reliable  $\kappa$  value, derived by  $F_{act}$  directly, in 1 second time resolution after stabilization for  $D_p$  scan measurement. Additionally, if we set a single particle size, we could derive  $\kappa$  value in 1 second time resolution. However, in this study, for calibration experiment, we use 1-min average data including stabilization time to calculate  $F_{act}$  value corresponding to each  $D_d$ .” (Line 119 – 126).

For inter-comparison experiment we set 19 dry diameters of 40 – 250 nm and select kappa value of close diameter in BS2-CCN measurement to the critical diameter obtained from DMA-CCN measurement. We mentioned this in Line 304 – 305 “Therefore, as shown in Fig. 9c, we used  $\kappa$  value of BS2-CCN measurement by selecting the particle diameter close to the average  $D_c$  of the DMA-CCN measurement for the inter-comparison.”

**Table R 1: Average and standard deviation value of  $F_{act}$  for each dry diameter.**

<b>Dp [nm]</b>	<b>Average <math>F_{act}</math></b>	<b>Standard deviation of <math>F_{act}</math></b>
<b>20</b>	0.00316866	0.00218781
<b>25</b>	0.00785123	0.00269424
<b>30</b>	0.03612815	0.00484231
<b>35</b>	0.05542066	0.00519961

40	0.26255714	0.01788727
45	0.47451548	0.0196648
50	0.61359299	0.01808588
55	0.71061904	0.0278038
60	0.76992656	0.02853376
65	0.80506852	0.02585054
70	0.84679062	0.0303469
75	0.88028529	0.02867314
80	0.91009636	0.02875085
85	0.91778563	0.03408703
90	0.93236908	0.03541124
95	0.95317282	0.03227177
100	0.94493573	0.04476325

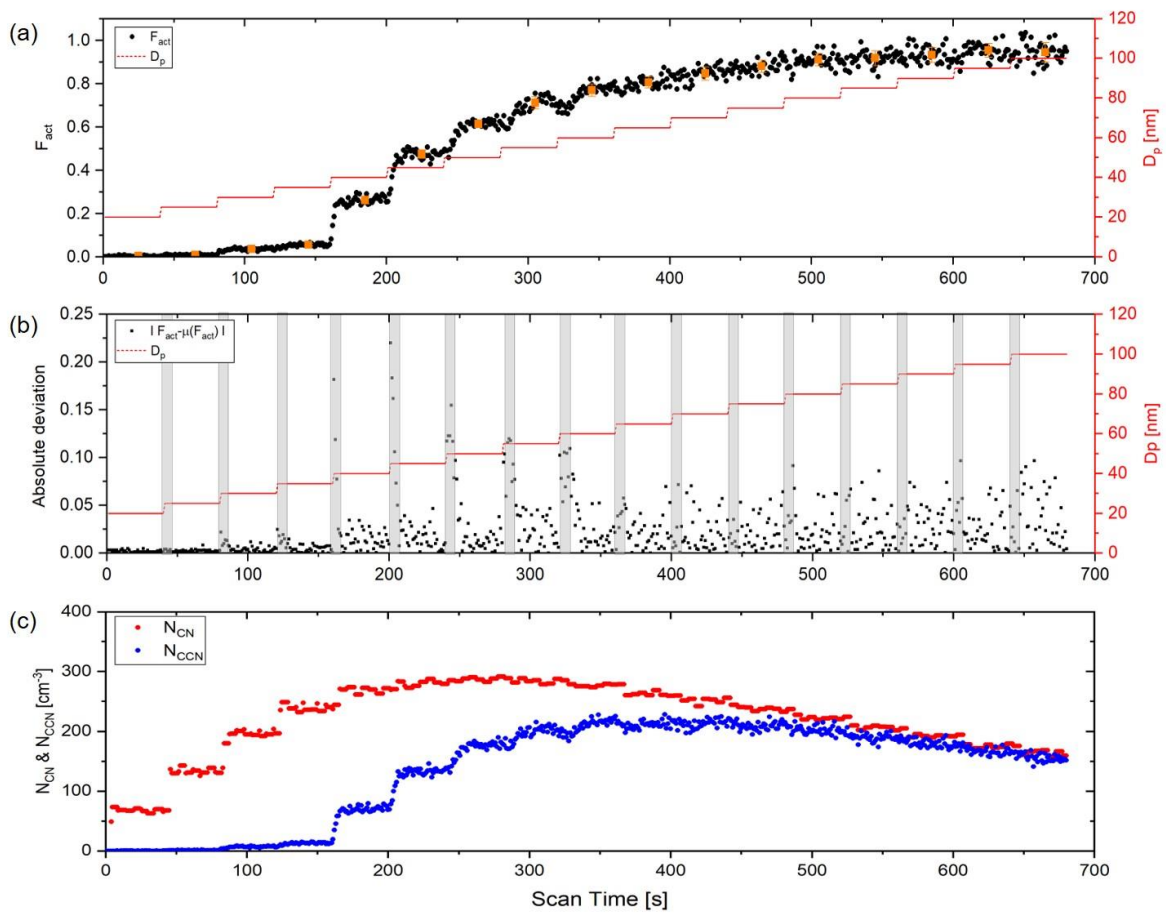


**Figure R 2: Exemplary  $D_p$  scan (20-100 nm) of lab generated ammonium sulfate. (a) 1 second data of activated fraction ( $F_{act}$ ), marked in black dot (left ordinate), particle diameter (red line, right ordinate). Average and standard deviation of each diameter (30-second average data except for 10 seconds of stabilization) are presented in orange square with bar. (b) Absolute deviation of  $F_{act}$  (black dot, left ordinate) and particle diameter (red line, right ordinate): The grey shaded box indicates the stabilization time (~10 seconds) of each particle diameter. (c) Particle number concentration ( $N_{CN}$ , red dot) and CCN number concentration ( $N_{CCN}$ , blue dot). Time resolution of each data point is 1 second and the particle diameter is changed every 40 seconds.  $S_{max}$  is set to be 10 K (0.8%).**

*Q3: The authors should discuss the new inlet in more detail. Were CFD simulations used to make sure that the flow is laminar? What are the limits of the angle to achieve laminar flow? For maximum impact, the authors should consider publish their CAD drawings under a non commercial use license so that others can more easily implement this technique. (Publication of the CAD drawing is not a requirement for publication in AMT, though in the reviewers opinion it should be).*

A: As the reviewer suggested, we conducted computational fluid dynamics (CFD) simulation with COMSOL Multiphysics (version 5.6). With our inlet design, laminar flow can be achieved regardless of the angle due to the low velocity. However, if the angle becomes too large (Figure R3b), flow separation occurs at the point where the aerosol and sheath flow meet, and there is a section where constant steady rotation of flow occurs. It means that the laminar flow cannot be achieved if there is no sheath flow, only aerosol flow. Everything above 15mm of cone length (65mm of the original design) doesn't show a separation of flowlines from the wall. We add the description of flow with the newly designed inlet in the main manuscript "According to the computational dynamic simulation result (COMSOL Multiphysics, version 5.6) of flow streamline and the relative particle concentration in Fig. A2, laminar flow inside the activation tube can be achieved with our new inlet design. Additionally, this new inlet allows for maintaining stable low sheath-to-aerosol flow ratios (SAR), for which monotonic  $F_{act} - S_{aerosol}$  relation can then be obtained." (Line 102-105) and add the figure of flow streamline and concentration (Figure R3a only) to support the description in Appendix A (Figure. A2).

Unfortunately, CAD drawing cannot be added in the manuscript. We showed the detailed front perspective view and Longitudinal sectional view of an embodiment of the newly designed inlet and the explanation of each part in Appendix A and Fig. A1. Compared to other instrument papers, including Fig.2 of Robert and Nenes (2005) for cloud condensation nuclei counter (CCNC), Jayne et al. (2000) for aerosol mass spectrometer (AMS), Fig.1 and Fig.2 of Pinterich et al. (2017) for a humidity-controlled fast integrated mobility spectrometer (HFIMS), we believe that our manuscript provides sufficient information on the concept and description of new measurement system as well as the design of new inlet. More detailed information of the newly designed inlet will be provided by the corresponding author (Dr. Hang Su, h.su@mpic.de) upon request and we are always welcome to collaborate.

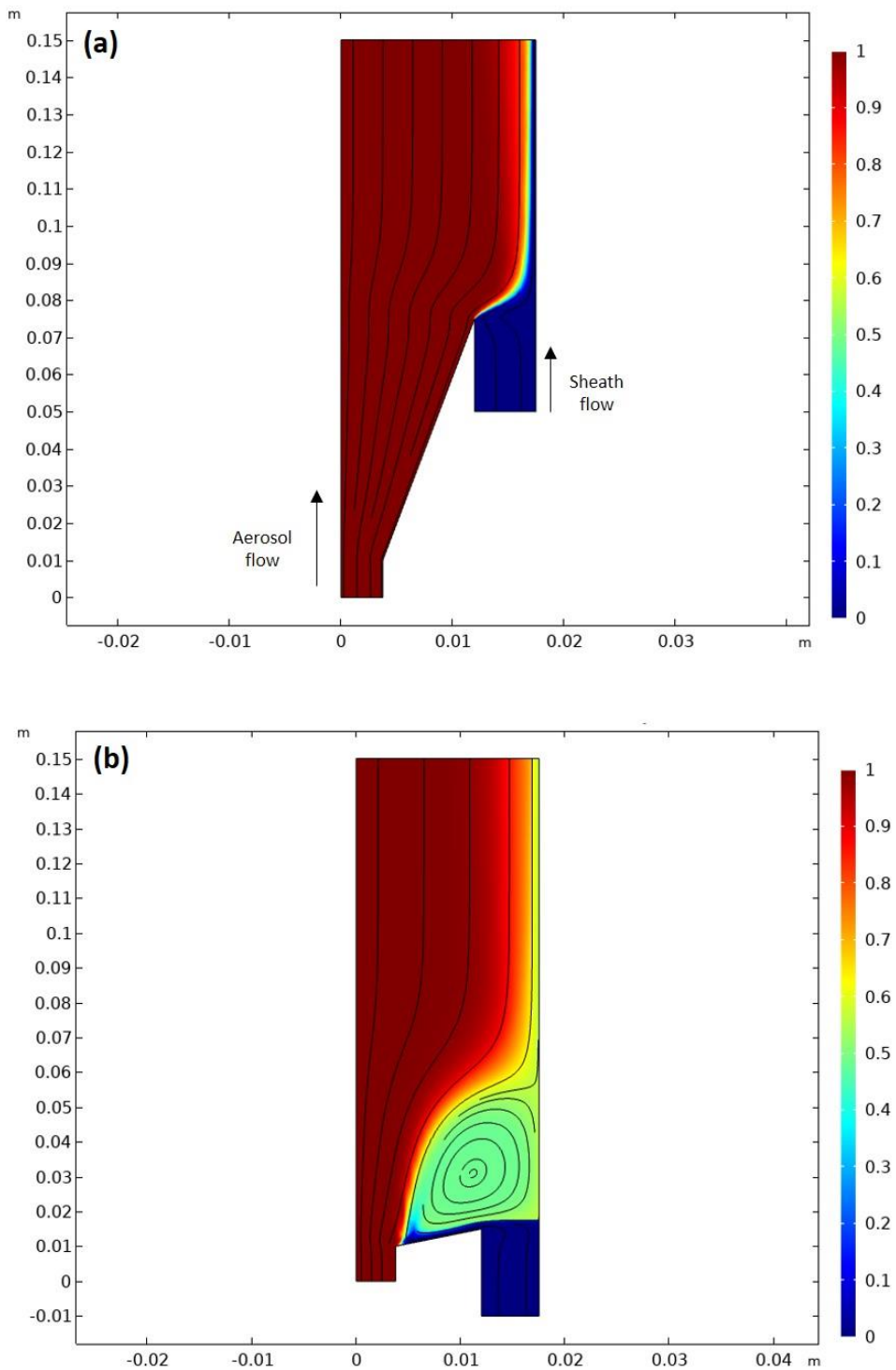


**Figure R 3. Results of computational fluid dynamics simulation with (a) original inlet design and (b) modified inlet design. A solid black line and the color bar indicate the flow streamline in the velocity field and the relative particle concentration [mol/m<sup>3</sup>], respectively. It is noted that the figure presents the half side of a longitudinal sectional view of Fig.A1(b) and the x and y axes represent the length of the inlet (units are meters). The aerosol and sheath flow go from the bottom (-y) to the top (+y).**

*Q4: “Data can be accessed by contacting the corresponding author. “: This is incompatible with the data policy of AMT.*

A: Following the data policy of AMT, we integrated the data of figures in the manuscript and uploaded the data on the Edmond, the open research data repository of the Max Planck Society. And, we add link for data and sentences “Data can be downloaded from Edmond, open research data repository of Max Planck Society (<https://edmond.mpg.de/imeji/collection/pohD2XdTlrMwzka7>), and raw data are available upon request from the corresponding author (h.su@mpic.de)” in Data Availability.

### **Other comments**

*Q5: Figure 3: The distribution doesn't peak at 50 nm as stated in the text.*

A: The peak diameter of the distribution on Figure 3 (now Figure 4) is 50 nm. Due to the x-axis, it is not clear to show the peak diameter. Therefore, we changed the x-axis of Fig.4 (a) and (b). Also, we had small mistake in caption. We changed value of  $\sigma_g$  from 1.4 to 1.5.

### **Reference**

J.T. Jayne, D.C. Leard, X. Zhang, P. Davidovits, K.A. Smith, C.E. Kolb, and D.R. Worsnop.: Development of an aerosol mass spectrometer for size and composition analysis of submicron particles, *Aerosol Sci. Technol.*, 33, 49-70, 2000.

Pinterich, T., Spielman, S. R., Wang, Y., Hering, S. V., and Wang, J.: A humidity-controlled fast integrated mobility spectrometer (HFIMS) for rapid measurements of particle hygroscopic growth, *Atmos. Meas. Tech.*, 10, 4915–4925, <https://doi.org/10.5194/amt-10-4915-2017>, 2017.

Roberts, G. C. and Nenes, A.: A Continuous-Flow Streamwise Thermal-Gradient CCN Chamber for Atmospheric Measurements', *Aerosol Science and Technology*, 39:3, 206 – 221, <https://doi.org/10.1080/027868290913988>, 2005.

Rose, D., Gunthe, S. S., Su, H., Garland, R. M., Yang, H., Berghof, M., Cheng, Y. F., Wehner, B., Achtert, P., Nowak, A., Wiedensohler, A., Takegawa, N., Kondo, Y., Hu, M., Zhang, Y., Andreae, M. O., and Pöschl, U.: Cloud condensation nuclei in polluted air and biomass burning smoke near the mega-city Guangzhou, China – Part 2: Size-resolved aerosol chemical composition, diurnal cycles, and externally mixed weakly CCN-active soot particles, *Atmos. Chem. Phys.*, 11, 2817–2836, doi:10.5194/acp-11- 2817-2011, 2011.